

Gene symbol	Description	Fold-change
ARHGAP26	Homo sapiens Rho GTPase activating protein 26 (ARHGAP26), transcript variant 1, mRNA [NM_015071]	-1.07
HPGD	Homo sapiens hydroxyprostaglandin dehydrogenase 15-(NAD) (HPGD), mRNA [NM_000860]	-1.07
CPN1	Homo sapiens carboxypeptidase N, polypeptide 1 (CPN1), mRNA [NM_001308]	-1.06
PPARGC1A	Homo sapiens peroxisome proliferator-activated receptor gamma, coactivator 1 alpha (PPARGC1A), mRNA [NM_013261]	-1.06
HLA-DPB1	Homo sapiens major histocompatibility complex, class II, DP beta 1 (HLA-DPB1), mRNA [NM_002121]	-1.06
BCMO1	Homo sapiens beta-carotene 15,15'-monooxygenase 1 (BCMO1), mRNA [NM_017429]	-1.05
PACSIN1	Homo sapiens protein kinase C and casein kinase substrate in neurons 1 (PACSIN1), mRNA [NM_020804]	-1.05
RIPK4	Homo sapiens receptor-interacting serine-threonine kinase 4 (RIPK4), mRNA [NM_020639]	-1.04
CEACAM6	Homo sapiens carcinoembryonic antigen-related cell adhesion molecule 6 (non-specific cross reacting antigen) (CEACAM6), mRNA [NM_002483]	-1.04
FGA	Homo sapiens fibrinogen alpha chain (FGA), transcript variant alpha, mRNA [NM_021871]	-1.04
GPR37	Homo sapiens G protein-coupled receptor 37 (endothelin receptor type B-like) (GPR37), mRNA [NM_005302]	-1.04
SLC23A2	Homo sapiens solute carrier family 23 (nucleobase transporters), member 2 (SLC23A2), transcript variant 2, mRNA [NM_203327]	-1.04
CDH17	Homo sapiens cadherin 17, LI cadherin (liver-intestine) (CDH17), mRNA [NM_004063]	-1.04
UPK1B	Homo sapiens uroplakin 1B (UPK1B), mRNA [NM_006952]	-1.03
SLC22A3	Homo sapiens solute carrier family 22 (extraneuronal monoamine transporter), member 3 (SLC22A3), mRNA [NM_021977]	-1.03
C4BPA	Homo sapiens complement component 4 binding protein, alpha (C4BPA), mRNA [NM_000715]	-1.03
C5orf23	Homo sapiens chromosome 5 open reading frame 23 (C5orf23), mRNA [NM_024563]	-1.03
HGD	Homo sapiens homogentisate 1,2-dioxygenase (homogentisate oxidase) (HGD), mRNA [NM_000187]	-1.03
CCND3	Homo sapiens cyclin D3 (CCND3), transcript variant 2, mRNA [NM_001760]	-1.02

Gene symbol	Description	Fold-change
RAP1GAP	Homo sapiens RAP1 GTPase activating protein (RAP1GAP), mRNA [NM_002885]	-1.02
TBXAS1	Homo sapiens thromboxane A synthase 1 (platelet) (TBXAS1), transcript variant TXS-II, mRNA [NM_030984]	-1.02
CPNE4	Homo sapiens copine IV (CPNE4), mRNA [NM_130808]	-1.01
MAP7	Homo sapiens microtubule-associated protein 7 (MAP7), mRNA [NM_003980]	-1.01
F5	Homo sapiens coagulation factor V (proaccelerin, labile factor) (F5), mRNA [NM_000130]	-1.01
SMC1A	Homo sapiens structural maintenance of chromosomes 1A (SMC1A), mRNA [NM_006306]	-1.01
FGFR3	Homo sapiens fibroblast growth factor receptor 3 (FGFR3), transcript variant 1, mRNA [NM_000142]	-1.01
SYT6	Homo sapiens synaptotagmin VI (SYT6), mRNA [NM_205848]	-1.01
PDZK1	Homo sapiens PDZ domain containing 1 (PDZK1), mRNA [NM_002614]	-1.00
NCALD	Homo sapiens neurocalcin delta (NCALD), transcript variant 7, mRNA [NM_001040630]	-1.00

Table S3 List of the Genes Up-regulated by 20 µg / mL of ZnCl₂.

Gene symbol	Description	Fold-change
MT1F*	Homo sapiens metallothionein 1F (MT1F), mRNA [NM_005949]	3.53
CXCL1	Homo sapiens chemokine (C-X-C motif) ligand 1 (melanoma growth stimulating activity, alpha) (CXCL1), mRNA [NM_001511]	1.87
MT2A*	Homo sapiens metallothionein 2A (MT2A), mRNA [NM_005953]	1.54
MT1G*	Homo sapiens metallothionein 1G (MT1G), mRNA [NM_005950]	1.53
C15orf48	Homo sapiens chromosome 15 open reading frame 48 (C15orf48), transcript variant 2, mRNA [NM_032413]	1.46
MT1A*	Homo sapiens metallothionein 1A (MT1A), mRNA [NM_005946]	1.45
ZDHHC21	Homo sapiens zinc finger, DHHC-type containing 21 (ZDHHC21), mRNA [NM_178566]	1.40
ANG	Homo sapiens angiogenin, ribonuclease, RNase A family, 5 (ANG), transcript variant 1, mRNA [NM_001145]	1.35
MT1H*	Homo sapiens metallothionein 1H (MT1H), mRNA [NM_005951]	1.34
CCL5	Homo sapiens chemokine (C-C motif) ligand 5 (CCL5), mRNA [NM_002985]	1.31
STT3B	Homo sapiens STT3, subunit of the oligosaccharyltransferase complex, homolog B (S. cerevisiae) (STT3B), mRNA [NM_178862]	1.31
MT1X*	Homo sapiens metallothionein 1X (MT1X), mRNA [NM_005952]	1.29
DHRS2*	Homo sapiens dehydrogenase/reductase (SDR family) member 2 (DHRS2), transcript variant 1, mRNA [NM_182908]	1.24
SCD	Homo sapiens stearoyl-CoA desaturase (delta-9-desaturase) (SCD), mRNA [NM_005063]	1.22
IL6	Homo sapiens interleukin 6 (interferon, beta 2) (IL6), mRNA [NM_000600]	1.20
GLB1L	Homo sapiens galactosidase, beta 1-like (GLB1L), mRNA [NM_024506]	1.18
JUP	Homo sapiens junction plakoglobin (JUP), transcript variant 1, mRNA [NM_002230]	1.14
ANPEP	Homo sapiens alanyl (membrane) aminopeptidase (ANPEP), mRNA [NM_001150]	1.12
HHIPL2	Homo sapiens HHIP-like 2 (HHIPL2), mRNA [NM_024746]	1.11
C16orf73	Homo sapiens chromosome 16 open reading frame 73 (C16orf73), mRNA [NM_152764]	1.10
MT1B*	Homo sapiens metallothionein 1B (MT1B), mRNA [NM_005947]	1.09

Gene symbol	Description	Fold-change
MAFK	Homo sapiens v-maf musculoaponeurotic fibrosarcoma oncogene homolog K (avian) (MAFK), mRNA [NM_002360]	1.08
NMB	Homo sapiens neuromedin B (NMB), transcript variant 1, mRNA [NM_021077]	1.06
ERAP2	Homo sapiens endoplasmic reticulum aminopeptidase 2 (ERAP2), transcript variant 1, mRNA [NM_022350]	1.05
ULK1	Homo sapiens unc-51-like kinase 1 (C. elegans) (ULK1), mRNA [NM_003565]	1.05
NNMT	Homo sapiens nicotinamide N-methyltransferase (NNMT), mRNA [NM_006169]	1.04
CRYAB	Homo sapiens crystallin, alpha B (CRYAB), mRNA [NM_001885]	1.03
SNX10	Homo sapiens sorting nexin 10 (SNX10), mRNA [NM_013322]	1.02
PDCD4	Homo sapiens programmed cell death 4 (neoplastic transformation inhibitor) (PDCD4), transcript variant 2, mRNA [NM_145341]	1.01

Table S4 List of the Genes Down-regulated by 20 µg / mL of ZnCl₂.

Gene symbol	Description	Fold-change	Gene symbol	Description	Fold-change
TMEM27	Homo sapiens transmembrane protein 27 (TMEM27), mRNA [NM_020665]	-1.66	KIF20A	Homo sapiens kinesin family member 20A (KIF20A), mRNA [NM_005733]	-1.08
QKI	Homo sapiens quaking homolog, KH domain RNA binding (mouse) (QKI), transcript variant 1, mRNA [NM_006775]	-1.44	ANXA3	Homo sapiens annexin A3 (ANXA3), mRNA [NM_005139]	-1.08
CPM	Homo sapiens carboxypeptidase M (CPM), transcript variant 1, mRNA [NM_001874]	-1.43	SET	Homo sapiens SET nuclear oncogene (SET), transcript variant 2, mRNA [NM_003011]	-1.07
BTN2A1	Homo sapiens butyrophilin, subfamily 2, member A1 (BTN2A1), transcript variant 2, mRNA [NM_078476]	-1.38	SLC27A2	Homo sapiens solute carrier family 27 (fatty acid transporter), member 2 (SLC27A2), mRNA [NM_003645]	-1.06
HSP90AA1	Homo sapiens heat shock protein 90kDa alpha (cytosolic), class A member 1 (HSP90AA1), transcript variant 2, mRNA [NM_005348]	-1.33	PTBP1	Homo sapiens polypyrimidine tract binding protein 1 (PTBP1), transcript variant 1, mRNA [NM_002819]	-1.06
UACA	Homo sapiens uveal autoantigen with coiled-coil domains and ankyrin repeats (UACA), transcript variant 2, mRNA [NM_001008224]	-1.32	UGCG	Homo sapiens UDP-glucose ceramide glucosyltransferase (UGCG), mRNA [NM_003358]	-1.06
FAM83D	Homo sapiens family with sequence similarity 83, member D (FAM83D), mRNA [NM_030919]	-1.32	SGK493	Homo sapiens protein kinase-like protein Sgk493 (SGK493), mRNA [NM_138370]	-1.05
LEPROT	Homo sapiens leptin receptor overlapping transcript (LEPROT), mRNA [NM_017526]	-1.28	NFE2L3	Homo sapiens nuclear factor (erythroid-derived 2)-like 3 (NFE2L3), mRNA [NM_004289]	-1.05
CENPA	Homo sapiens centromere protein A (CENPA), transcript variant 1, mRNA [NM_001809]	-1.27	TROVE2	Homo sapiens TROVE domain family, member 2 (TROVE2), transcript variant 1, mRNA [NM_001042369]	-1.04
PABPC3	Homo sapiens poly(A) binding protein, cytoplasmic 3 (PABPC3), mRNA [NM_030979]	-1.22	MGC3207	Homo sapiens translation initiation factor eIF-2B subunit alpha/beta/delta-like protein (MGC3207), transcript variant 1, mRNA [NM_001031727]	-1.04
CAV3	Homo sapiens caveolin 3 (CAV3), transcript variant 1, mRNA [NM_033337]	-1.20	LMNB2	Homo sapiens lamin B2 (LMNB2), mRNA [NM_032737]	-1.03
CPA4	Homo sapiens carboxypeptidase A4 (CPA4), mRNA [NM_016352]	-1.19	PRPS2	Homo sapiens phosphoribosyl pyrophosphate synthetase 2 (PRPS2), transcript variant 1, mRNA [NM_001039091]	-1.03
IRS1	Homo sapiens insulin receptor substrate 1 (IRS1), mRNA [NM_005544]	-1.18	IGFBP7	Homo sapiens insulin-like growth factor binding protein 7 (IGFBP7), mRNA [NM_001553]	-1.03
BAT2D1	Homo sapiens BAT2 domain containing 1 (BAT2D1), mRNA [NM_015172]	-1.17	CCNB1	Homo sapiens cyclin B1 (CCNB1), mRNA [NM_031966]	-1.00
MYLK	Homo sapiens myosin light chain kinase (MYLK), transcript variant 1, mRNA [NM_053025]	-1.15			
PL-5283	Homo sapiens PL-5283 protein (PL-5283), mRNA [NM_001130929]	-1.12			
KIAA0802	Homo sapiens KIAA0802 (KIAA0802), mRNA [NM_015210]	-1.12			
DDX6	Homo sapiens DEAD (Asp-Glu-Ala-Asp) box polypeptide 6 (DDX6), mRNA [NM_004397]	-1.11			
C8orf38	Homo sapiens chromosome 8 open reading frame 38 (C8orf38), mRNA [NM_152416]	-1.11			
GOSR1	Homo sapiens golgi SNAP receptor complex member 1 (GOSR1), transcript variant 1, mRNA [NM_004871]	-1.10			
AK3	Homo sapiens adenylate kinase 3 (AK3), nuclear gene encoding mitochondrial protein, mRNA [NM_016282]	-1.09			
ZNF319	Homo sapiens zinc finger protein 319 (ZNF319), mRNA [NM_020807]	-1.08			
PDCD5	Homo sapiens programmed cell death 5 (PDCD5), mRNA [NM_004708]	-1.08			

乳幼児が誤飲する可能性のある金属製アクセサリからの有害 8 元素の溶出

伊佐間和郎,* 河上強志, 西村哲治†

Migration of Eight Harmful Elements from Metal Accessories That Infants May Swallow by Mistake

Kazuo Isama,* Tsuyoshi Kawakami, and Tetsuji Nishimura†

Division of Environmental Chemistry, National Institute of Health Sciences; 1-18-1 Kamiyoga, Setagaya-ku, Tokyo 158-8501, Japan.

(Received April 19, 2012; Accepted May 22, 2012)

The International Standard ISO 8124-3:2010 “Safety of toys—Part 3: Migration of certain elements” controls the levels of migrated eight harmful elements (antimony, arsenic, barium, cadmium, chromium, lead, mercury and selenium) from infants toys. Moreover, the Japanese Food Sanitation Law controls the levels of migrated lead from metal accessory toys. However, the levels of migrated harmful elements from metal accessories that are not infants toys are not controlled, since they are not covered by the ISO Standard or the Food Sanitation Law. Therefore, we investigated the level of eight harmful elements migrated from metal accessories that infants may swallow by mistake. The extraction test of ISO 8124-3:2010 was executed in 117 products (total 184 specimens), and the concentration of these eight elements was measured by inductively coupled plasma mass spectroscopy (ICP-MS). As a result, 28 and one products released lead and cadmium beyond the maximum acceptable levels of the ISO standard, respectively. Metal accessories that infants may swallow by mistake should ideally not release harmful elements such as lead and cadmium.

Key words—lead; cadmium; metal accessory; ISO 8124-3:2010; inductively coupled plasma mass spectroscopy (ICP-MS)

緒 言

国際標準化機構 (International Organization for Standardization, ISO) は, 玩具安全規格 (ISO 8124-3:2010) を制定し, 6 歳以下の幼児用玩具を対象として, 玩具材料毎にアンチモン, ヒ素, バリウム, カドミウム, クロム, 鉛, 水銀及びセレンの溶出限度値を定めている (Table 1).¹⁾ また, わが国の食品衛生法のおもちゃの規格基準では, 金属製アクセサリ玩具のうち, 乳幼児が飲み込むおそれがあるものについて, 鉛の溶出量は 90 µg/g 以下でなければならないと規定している. しかしながら, 乳幼児が飲み込むおそれがある大きさでも, 金属製アクセサリ玩具に該当しない金属製アクセサリ等には, 鉛その他の有害元素の溶出量に係る基準はない.

平成 18 年に米国で起きた鉛を高濃度含有するブ

レスレットを誤飲した幼児が鉛中毒で死亡した事故を受けて, 平成 18 年及び平成 19 年に金属製アクセサリ類等及びアクセサリ類を除く金属製品を対象にカドミウム及び鉛の含有量及び溶出量が調査された.²⁻⁵⁾ その結果, 一部の製品から一定量を超える鉛の溶出が確認されたため, 厚生労働省は注意喚起等を行った.^{6,7)} ところが, 再び米国で一部の子供用金属製アクセサリからカドミウムが溶出することが確認され, 平成 22 年及び平成 23 年に消費者庁及び国民生活センターが輸入された子供用金属製アクセサリを対象にカドミウム及び鉛の溶出量を調

Table 1. Maximum Acceptable Element Migration from Toy Materials Required by ISO 8124-3:2010

Toy material	Element (mg/kg)							
	Sb	As	Ba	Cd	Cr	Pb	Hg	Se
Any toy material except modelling clay and finger paint	60	25	1000	75	60	90	60	500
Modelling clay and finger paint	60	25	250	50	25	90	25	500

The authors declare no conflict of interest.
 国立医薬品食品衛生研究所生活衛生化学部
 現所属: †帝京平成大学薬学部
 *e-mail: isama@nihs.go.jp

査した。その結果、一部の製品から一定量を超える鉛の溶出が認められ、^{8,9)} 消費者庁及び国民生活センターは注意喚起を行った。¹⁰⁻¹³⁾ また、平成 22 年度家庭用品等に係る健康被害病院モニター報告によると、小児の誤飲事故のうち、約 5% が金属製品によるものであった。¹⁴⁾ さらに、東京都のヒヤリ・ハット調査でも、金属製と推察されるアクセサリ（ヘアピン、指輪など）及び家庭用品（携帯ストラップ、キーホルダーなど）を乳幼児が「誤飲しそうになった」又は「誤飲した」という回答が報告されている。¹⁵⁾ 鉛その他の有害元素を含有した製品を乳幼児が誤飲した場合、健康被害を起こす可能性がある。そこで、乳幼児が誤飲する可能性のある金属製アクセサリ等を対象に、ISO 玩具安全規格で規制されている有害 8 元素（アンチモン、ヒ素、バリウム、カドミウム、クロム、鉛、水銀及びセレン）の溶出量について、フォローアップ調査を実施した。

方 法

1. 試料 平成 23 年 8 月から 11 月までに、東京都内の複数の小売店で、乳幼児が誤飲する可能性のある大きさの金属製アクセサリ等 117 製品を購入した（Table 2）。製品は千円以下で購入可能な安価なものを選び、購入に際して製造国は考慮しなかった。製品の表示から、中国製 43 製品、韓国製 15 製品、日本製 8 製品及び不明 51 製品であった。また、乳幼児が誤飲する可能性のある大きさは、食品

Table 2. Number of Products and Specimens by the Commodity Classification

Commodity classification	Number of products	Number of specimens
Straps	30	65
Accessory parts	21	22
Hairpins	20	20
Necklaces	17	42
Charms	9	9
Rings	6	6
Fastener straps	4	4
Bracelets	3	8
Earrings	3	3
Cufflinks	2	2
Pin badges	1	2
Buttons	1	1
Total	117	184

衛生法に基づく「食品、添加物等の規格基準 第 4 おもちゃ」で規定する寸法を持つ容器内に圧縮しない状態で置いたときに収まるものとした。¹⁶⁾ 製品又は容易に分離可能な部品を検体とした（計 184 検体）。

2. 試薬 有害金属測定用塩酸（和光純薬工業株式会社）を、純水製造装置 Elix UV 5（日本ミリポア株式会社）及び超純水製造装置 Milli-Q Synthesis A10（日本ミリポア株式会社）を用いて製造した超純水で希釈し、溶出試験用の 0.07 mol/L 塩酸を調製した。アンチモン、ヒ素、バリウム、カドミウム、クロム、鉛、水銀及びセレンの各 1000 mg/L 標準液（和光純薬工業株式会社）並びに 0.07 mol/L 塩酸を用いて、当該 8 元素の 10 mg/L 混合溶液を調製した。この混合溶液を 0.07 mol/L 塩酸で段階希釈し、検量線作成用の混合標準液を調製した。イットリウム及びタリウムの 1 µg/L 溶液（アジレント・テクノロジー株式会社）を内標準溶液とした。

3. 装置及び測定条件 誘導結合プラズマ質量分析（ICP-MS）には、Agilent 7500ce ORS ICP-MS（アジレント・テクノロジー株式会社）を使用した。

ICP-MS の測定条件は、高周波出力：1500 W、プラズマガス：Ar 15 L/min、キャリアガス：Ar 0.7 L/min、メイクアップガス：Ar 0.33 L/min、コリジョンガス：He 5 mL/min、サンプリング位置：7.8 mm、スプレーチャンバー温度：2°C、積分時間：0.1 s/element（セレンを除く 7 元素）及び 1 s/element（セレン）、測定回数：3 times とした。測定元素及び内標準元素並びにそれらの測定質量数 (m/z) を Table 3 に示した。

4. 試験溶液の調製 検体の質量を量り、内径約 40 mm のポリプロピレン製容器に入れ、37°C に加温した溶出試験用 0.07 mol/L 塩酸を試料が浸漬するまで加えて蓋をし、遮光して 37°C で 2 時間放置した後、ポアサイズ 0.45 µm のメンブレンフィルター（ザルトリウス・メカトロニクス・ジャパン株

Table 3. Determined Elements, Internal Standards and Their Mass Numbers

Determined element	Sb	As	Ba	Cd	Cr	Pb	Hg	Se
Mass number (m/z)	121	75	137	111	53	208	202	82
Internal standard	Y	Y	Y	Y	Y	Tl	Tl	Y
Mass number (m/z)	89	89	89	89	89	205	205	89

式会社)でろ過し、試験溶液とした。なお、検量線の範囲に収まるように、必要に応じて0.07 mol/L塩酸を用いて100倍から10000倍に希釈した。

5. 定量 混合標準液のICP-MS測定から、内標準法により検量線を作成した。作成した検量線から試験溶液中の各測定元素の濃度を求め、次式により試験に供した検体1 kg当たりの溶出量 (mg/kg)を算出した。

$$\text{溶出量 (mg/kg)} = \frac{\text{試験溶液中の濃度 (mg/L)} \times \text{試験溶液の容量 (L)}}{\text{検体質量 (kg)}}$$

食品衛生法のおもちゃの規格基準及びISO玩具安全規格では、試験法の正確化のため、分析補正值により分析値を補正することが規定されているが、今回の調査は食品衛生法のおもちゃの規格基準及びISO玩具安全規格への適否を判定することが目的ではないので、分析補正值は考慮しなかった。また、ISO玩具安全規格では、溶出限度値の1/10を測定下限値としているが、今回は溶出限度値の1/100を測定下限値とした。なお、試験溶液のICP-MS測定における検出下限値及び定量下限値は、ブランク値の標準偏差のそれぞれ3倍及び10倍とした。¹⁷⁾

結 果

1. ICP-MS 測定の精度 ICP-MS測定における各測定元素の検出下限値、定量下限値及びバックグラウンド相当濃度 (BEC) をTable 4に示した。今回のICP-MS測定における検出下限値は、いずれの測定元素についてもISO玩具安全規格の溶出限度値 (Table 1) のおよそ1/100000に相当する濃度であり、試験溶液の測定にICP-MSを用いることは妥当である。

2. 市販製品の溶出試験 鉛、カドミウム及びクロムについて、商品分類別のISO玩具安全規格の溶出限度値 (Table 1) の1/10以下の製品数 (検体数)、溶出限度値の1/10を超え溶出限度値以下の

製品数 (検体数) 及び溶出限度値を超えた製品数 (検体数) をそれぞれTable 5-7に示した。また、測定元素のいずれかが溶出限度値 (Table 1) を超えた製品 (検体) 及びそれらの各測定元素の溶出量をそれぞれFig. 1及びTable 8に示した。ストラップ、アクセサリパーツ、チャーム、ヘアピン、ネックレスなど28製品 (30検体) が溶出限度値 (90 mg/kg) を超える鉛を溶出し、さらに26製品 (31検体) が溶出限度値の1/10を超え溶出限度値以下の鉛を溶出した (Table 5)。チャーム (No. 16; 569 mg/kg)、アクセサリパーツの飾り (No. 15-1; 523 mg/kg)、ストラップの金具 (No. 1-2; 501 mg/kg) 及びアクセサリパーツ (No. 14; 461 mg/kg) が溶出限度値 (90 mg/kg) の5倍を超える鉛を溶出した (Table 8)。また、ブレスレット (No. 26; 160 mg/kg) の1製品 (1検体) が溶出限度値 (75 mg/kg) を超えるカドミウムを溶出し (Table 8)、さらに5製品 (5検体) が溶出限度値の1/10を超え溶出限度値以下のカドミウムを溶出した (Table 6)。溶出限度値 (60 mg/kg) を超えるクロムを溶出した製品はなく、6製品 (7検体) が溶出限度値の1/10を超え溶出限度値以下のクロムを溶出した (Table 7)。なお、溶出限度値の1/10を超えるアンチモン、ヒ素、バリウム、水銀及びセレンを溶出した製品 (検体) はなかった。

考 察

食品衛生法は、飲食に起因する衛生上の危害の発生の防止を目的とするものであるが、乳幼児玩具には、乳幼児が口に接触することをその本質とするおもちゃが存在すること及び一定年齢の乳幼児は身の周りにあるものを口に入れるという性質があること等の理由から、同法に基づき、乳幼児が接触することによりその健康を損なうおそれがあるものとして厚生労働大臣が指定する玩具 (指定おもちゃ) が規定され、必要な規格及び製造基準が設定されてい

Table 4. Detection Limits, Determination Limits and Background Equivalent Concentrations (BEC) in ICP-MS

Element	Sb	As	Ba	Cd	Cr	Pb	Hg	Se
Detection limit ^a (ng/L)	12.8	21.3	15.4	3.08	38.8	89.3	9.65	32.2
Determination limit ^b (ng/L)	42.7	71.1	51.4	10.3	129	298	32.2	107
BEC (ng/L)	77.1	14.4	52.2	8.11	197	593	84.6	104

^a Three times of the standard deviation of a blank. ^b Ten times of the standard deviation of a blank.

Table 5. Migrations of Lead by the Commodity Classification

Commodity classification	Number of products (Number of specimens)	≤ 9 mg/kg	9 mg/kg <, ≤ 90 mg/kg	90 mg/kg ^a <
Straps	30 (65)	13 (47)	7 (7)	10 (11)
Accessory parts	21 (22)	12 (12)	4 (4)	5 (6)
Hairpins	20 (20)	15 (15)	2 (2)	3 (3)
Necklaces	17 (42)	7 (29)	7 (10)	3 (3)
Charms	9 (9)	4 (4)	1 (1)	4 (4)
Rings	6 (6)	1 (1)	4 (4)	1 (1)
Fastener straps	4 (4)	4 (4)	0 (0)	0 (0)
Bracelets	3 (8)	1 (4)	1 (3)	1 (1)
Earrings	3 (3)	3 (3)	0 (0)	0 (0)
Cufflinks	2 (2)	2 (2)	0 (0)	0 (0)
Pin badges	1 (2)	1 (2)	0 (0)	0 (0)
Buttons	1 (1)	0 (0)	0 (0)	1 (1)
Total	117 (184)	63 (123)	26 (31)	28 (30)
Frequency (%)	100 (100)	54 (67)	22 (17)	24 (16)

^a Maximum acceptable migration of lead from toy materials required by ISO 8124-3:2010.

Table 6. Migrations of Cadmium by the Commodity Classification

Commodity classification	Number of products (Number of specimens)	≤ 7.5 mg/kg	7.5 mg/kg <, ≤ 75 mg/kg	75 mg/kg ^a <
Straps	30 (65)	30 (65)	0 (0)	0 (0)
Accessory parts	21 (22)	20 (21)	1 (1)	0 (0)
Hairpins	20 (20)	20 (20)	0 (0)	0 (0)
Necklaces	17 (42)	14 (39)	3 (3)	0 (0)
Charms	9 (9)	9 (9)	0 (0)	0 (0)
Rings	6 (6)	5 (5)	1 (1)	0 (0)
Fastener straps	4 (4)	4 (4)	0 (0)	0 (0)
Bracelets	3 (8)	3 (8)	0 (0)	1 (1)
Earrings	3 (3)	3 (3)	0 (0)	0 (0)
Cufflinks	2 (2)	2 (2)	0 (0)	0 (0)
Pin badges	1 (2)	1 (2)	0 (0)	0 (0)
Buttons	1 (1)	1 (1)	0 (0)	0 (0)
Total	117 (184)	112 (179)	5 (5)	1 (1)
Frequency (%)	100 (100)	95 (96)	4 (3)	1 (1)

^a Maximum acceptable migration of cadmium from toy materials required by ISO 8124-3:2010.

る。平成 20 年 3 月 31 日に、食品衛生法に基づく「食品、添加物等の規格基準」の「おもちゃ又はその原材料の規格」が改正され、金属製アクセサリ玩具のうち、乳幼児が飲み込むおそれがあるものについて、鉛の溶出量は 90 $\mu\text{g/g}$ 以下でなければならないという規定が追加された。^{18,19)}しかし、金属製アクセサリ玩具に該当しない金属製アクセサリ等の金属製品から溶出する鉛その他の有害元素は規制されておらず、乳幼児が誤飲した場合の健康影響が懸念される。

今回調査した乳幼児が飲み込むおそれがある金属製アクセサリ等 117 製品のうち、いずれかの元素が ISO 玩具安全規格の溶出限度値 (Table 1) を超えたのは 29 製品あり、検出頻度は 25%であった。特に、カドミウムを溶出した 1 製品を除き、鉛を溶出した製品が多かった。鉛は金属製品以外の家庭用品等に含有したり、それらから溶出したりすることも報告されている。例えば、子供用髪留めの塗膜から食品衛生法の規格基準を超える鉛の溶出が確認され、食品衛生法の対象外の製品であるが、国内販売

Table 7. Migrations of Chromium by the Commodity Classification

Commodity classification	Number of products (Number of specimens)	≤ 6 mg/kg	6 mg/kg <, ≤ 60 mg/kg	60 mg/kg ^a <
Straps	30(65)	29(63)	1(2)	0(0)
Accessory parts	21(22)	16(17)	5(5)	0(0)
Hairpins	20(20)	20(20)	0(0)	0(0)
Necklaces	17(42)	17(42)	0(0)	0(0)
Charms	9(9)	9(9)	0(0)	0(0)
Rings	6(6)	6(6)	0(0)	0(0)
Fastener straps	4(4)	4(4)	0(0)	0(0)
Bracelets	3(8)	3(8)	0(0)	0(0)
Earrings	3(3)	3(3)	0(0)	0(0)
Cufflinks	2(2)	2(2)	0(0)	0(0)
Pin badges	1(2)	1(2)	0(0)	0(0)
Buttons	1(1)	20(20)	0(0)	0(0)
Total	117(184)	111(177)	6(7)	0(0)
Frequency (%)	100(100)	95(96)	5(4)	0(0)

^a Maximum acceptable migration of chromium from toy materials required by ISO 8124-3:2010.

Table 8. Migrations of Eight Elements from Products at Levels More than the Maximum Acceptable Levels of ISO 8124-3:2010

No.	Product	Specimen	Element (mg/kg)								
			Sb	As	Ba	Cd	Cr	Pb	Hg	Se	
1-1	Strap	decoration	nd ^b	nd	nd	nd	nd	nd	<u>136</u> ^c	nd	nd
1-2		fitting	nd	nd	nd	0.764	nd	<u>501</u>	nd	nd	
2	Strap	fitting	nd	nd	nd	1.07	nd	<u>418</u>	nd	nd	
3	Strap	fitting	nd	nd	nd	nd	nd	<u>428</u>	nd	nd	
4	Strap	fitting	nd	nd	nd	nd	nd	<u>125</u>	nd	nd	
5	Strap	decoration	nd	nd	nd	nd	nd	<u>167</u>	nd	nd	
6	Strap	decoration	nd	nd	nd	nd	nd	<u>368</u>	nd	nd	
7	Strap	fitting	nd	nd	nd	nd	nd	<u>104</u>	nd	nd	
8	Strap	decoration	nd	nd	nd	nd	nd	<u>218</u>	nd	nd	
9	Strap	decoration	nd	nd	nd	nd	nd	<u>252</u>	nd	nd	
10	Strap	decoration	nd	nd	nd	nd	nd	<u>145</u>	nd	nd	
11	Accessory part	— ^a	nd	nd	nd	nd	nd	<u>123</u>	nd	nd	
12	Accessory part	—	nd	nd	nd	21.3	nd	<u>241</u>	nd	nd	
13	Accessory part	—	nd	nd	nd	1.52	nd	<u>129</u>	nd	nd	
14	Accessory part	—	nd	nd	nd	1.24	nd	<u>461</u>	nd	nd	
15-1	Accessory part	decoration	nd	nd	nd	2.23	nd	<u>523</u>	nd	nd	
15-2		decoration	nd	nd	nd	1.50	nd	<u>312</u>	nd	nd	
16	Charm	—	nd	nd	nd	nd	nd	<u>569</u>	nd	nd	
17	Charm	—	nd	nd	nd	nd	nd	<u>296</u>	nd	nd	
18	Charm	—	nd	nd	nd	2.24	nd	<u>296</u>	nd	nd	
19	Charm	—	nd	nd	nd	1.44	nd	<u>330</u>	nd	nd	
20	Hairpin	—	nd	nd	nd	nd	nd	<u>166</u>	nd	nd	
21	Hairpin	—	nd	nd	nd	nd	nd	<u>112</u>	nd	nd	
22	Hairpin	—	nd	nd	nd	nd	nd	<u>145</u>	nd	nd	
23	Necklace	chain	nd	nd	nd	nd	nd	<u>200</u>	nd	nd	
24	Necklace	decoration	nd	nd	nd	nd	nd	<u>107</u>	nd	nd	
25	Necklace	decoration	nd	nd	nd	1.63	nd	<u>187</u>	nd	nd	
26	Bracelet	decoration	nd	nd	nd	<u>160</u>	nd	0.680	nd	nd	
27	Bracelet	decoration	nd	nd	nd	1.14	nd	<u>133</u>	nd	nd	
28	Ring	—	nd	nd	nd	1.15	nd	<u>139</u>	nd	nd	
29	Button	—	nd	nd	nd	nd	nd	<u>139</u>	nd	nd	

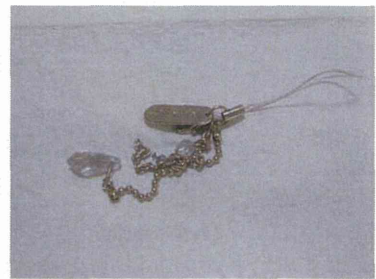
^a Tested the whole product. ^b Less than and equal to 1/100 of the maximum acceptable levels of ISO 8124-3:2010. ^c The underline shows the migrations at levels more than the maximum acceptable levels of ISO 8124-3:2010.



No. 1-1 (decoration), -2 (fitting)



No. 2



No. 3



No. 4



No. 5



No. 6



No. 7



No. 8



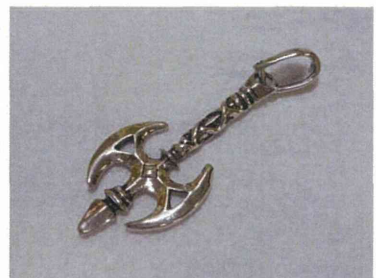
No. 9



No. 10



No. 11



No. 12



No. 13



No. 14



No. 15-1 (right), -2 (left)

Fig. 1. Products That Released Lead at a Level More than the Maximum Acceptable Level of ISO 8124-3:2010



No. 16



No. 17



No. 18



No. 19



No. 20



No. 21



No. 22



No. 23



No. 24



No. 25



No. 26



No. 27



No. 28



No. 29

Fig. 1. (Continued)

業者は自主的に回収した。^{20,21)} また、われわれも乳幼児が飲み込むおそれがある家庭用品の塗膜²²⁾及び合成樹脂製家庭用品¹⁶⁾の一部から鉛が溶出することを確認している。さらに、一部のレジ袋は最大25000 mg/kg、平均310 mg/kgの鉛を含有することが報告され、幼児がレジ袋を舐めたり飲み込んだりした場合の健康影響が懸念されている。²³⁾

鉛は中枢神経障害、腎機能障害、生殖機能障害及び造血器障害を生じる有害金属元素の1つであり、特に、乳幼児に対しては、一定レベル以上の血中濃度で、知能や神経の発達に有害な影響を与える可能性がある。^{24,25)} 米国疾病予防管理センター (Centers for Disease Control and Prevention) は、小児の血中鉛濃度の許容値を10 $\mu\text{g}/\text{dL}$ と定めている。²⁶⁾ さらに、米国消費者製品安全委員会 (The U.S. Consumer Product Safety Commission, CPSC) は、急性的暴露によって小児の血中鉛濃度が10 $\mu\text{g}/\text{dL}$ を超過するのを避けるため、短期間に175 μg を超える鉛を摂取することがないように勧告している。²⁷⁾ 今回調査した117製品(184検体)について、製品(検体)1個当たりの鉛の溶出量を算出した (Table 9)。ストラップ、アクセサリパーツ、ネックレスなど36製品(41検体)が製品(検体)1個当たり175 μg を超える鉛を溶出し、最大値はアクセサリパーツ (No. 14) の5904 μg であった。これらを小児が誤飲すると、米国CPSCの勧告 (175 μg)

を超える量の鉛を摂取する可能性があり、安全性に問題があると考えられる。

平成18年に実施した調査³⁾は、米国CPSCが規定した試験法²⁸⁾に準じ、鉛含有量が0.06%を超えた製品は鉛溶出量を175 μg 以下とする当時の暫定指針²⁷⁾に基づいて判定した。その結果、金属製アクセサリ一類等140製品のうち、鉛含有量が0.06%を超えたのは90製品であった。³⁾ さらに、鉛含有量が0.06%を超え、乳幼児が誤飲するおそれのある66製品のうち、鉛溶出量が175 μg を超えたのは39製品であった。³⁾ 米国CPSC指針の溶出試験とISO玩具安全規格の溶出試験は試験条件が異なり、一般に米国CPSC指針の溶出試験の方が鉛の溶出力が高い傾向にある。²⁹⁾ これらを考慮すると、わが国で市販されている金属製アクセサリ等において、高濃度の鉛を溶出する製品の割合は平成18年から現在までほとんど改善されていないと考えられる。乳幼児が誤飲する可能性のある金属製アクセサリ等の金属製品は、鉛やカドミウムなどの有害元素を溶出しないことが望ましく、これらの有害元素の溶出量を低減する努力が必要であろう。

米国では、2009年8月までに、子供用製品の鉛含有量を600 mg/kgから300 mg/kgに、子供用製品に使用される塗料及び塗膜の鉛含有量を600 mg/kgから90 mg/kgに、それぞれ低減するように規制が強化された。³⁰⁾ さらに、2011年8月までに、子供用

Table 9. Migrations of Lead per Product or per Specimen by the Commodity Classification

Commodity classification	Number of products (Number of specimens)	$\leq 175 \mu\text{g}$	$175 \mu\text{g}^{\text{a}} <, \leq 1750 \mu\text{g}$	$1750 \mu\text{g} <$
Straps	30 (65)	19 (53)	11 (12)	0 (0)
Accessory parts	21 (22)	13 (13)	5 (6)	3 (3)
Hairpins	20 (20)	17 (17)	3 (3)	0 (0)
Necklaces	17 (42)	12 (36)	5 (6)	0 (0)
Charms	9 (9)	5 (5)	4 (4)	0 (0)
Rings	6 (6)	4 (4)	2 (2)	0 (0)
Fastener straps	4 (4)	4 (4)	0 (0)	0 (0)
Bracelets	3 (8)	1 (4)	2 (4)	0 (0)
Earrings	3 (3)	3 (3)	0 (0)	0 (0)
Cufflinks	2 (2)	2 (2)	0 (0)	0 (0)
Pin badges	1 (2)	1 (2)	0 (0)	0 (0)
Buttons	1 (1)	0 (0)	1 (1)	0 (0)
Total	117(184)	81(143)	33(38)	3(3)
Frequency (%)	100(100)	69 (77)	28(21)	3(2)

^a Maximum acceptable migration of lead from children's metal jewelries by CPSC policy.

製品の鉛含有量を 100 mg/kg まで低減するように規制がより強化された。³⁰⁾ わが国では、平成 18 年以降、鉛等を含有する金属製アクセサリ一類の安全対策として、消費者等への注意喚起、医療関係者への情報提供及び業者団体への指導を行ってきた。^{4-13,25)} しかし、乳幼児の誤飲事故は後を絶たず、^{14,15)} 製品の改善も認められなかったことから、金属製アクセサリ等の誤飲による乳幼児の健康被害を防止するため、わが国でもさらに踏み込んだ対策が望まれる。

REFERENCES

- 1) International Organization for Standardization (ISO), "Safety of toys—Part 3: Migration of certain elements," ISO 8124-3:2010 (E), Switzerland, 2010.
- 2) Consumer Safety Section, Consumer Affairs Division, Bureau of Citizens and Cultural Affairs, Tokyo Metropolitan Government, *Ta-shikana Me*, **241**, 40-42 (2006).
- 3) Office of Chemical Safety, Evaluation and Licensing Division, Pharmaceutical and Food Safety Bureau, Ministry of Health, Labour and Welfare: <http://www.mhlw.go.jp/shingi/2006/06/dl/s0613-7g.pdf>, cited 19 April, 2012.
- 4) Isama K., Kaniwa M., Tsuchiya T., *Jpn. J. Toxicol.*, **19**, 409-411 (2006).
- 5) Isama K., Kaniwa M., Tsuchiya T., *Jpn. J. Toxicol.*, **21**, 393-395 (2008).
- 6) Office of Chemical Safety, Evaluation and Licensing Division, Pharmaceutical and Food Safety Bureau, Ministry of Health, Labour and Welfare: <http://www.mhlw.go.jp/topics/2006/03/tp0308-1.html>, cited 19 April, 2012.
- 7) Office of Chemical Safety, Evaluation and Licensing Division, Pharmaceutical and Food Safety Bureau, Ministry of Health, Labour and Welfare, *Jpn. J. Toxicol.*, **20**, 146-147 (2007).
- 8) National Consumer Affairs Center of Japan: http://www.kokusen.go.jp/test/data/s_test/n-20100325_1.html, cited 19 April, 2012.
- 9) National Consumer Affairs Center of Japan: http://www.kokusen.go.jp/test/data/s_test/n-20110810_1.html, cited 19 April, 2012.
- 10) Consumer Affairs Agency, Government of Japan: http://www.caa.go.jp/adjustments/pdf/100325adjustments_1.pdf, cited 19 April, 2012.
- 11) Products Testing Department, National Consumer Affairs Center of Japan, *Gekkan Koku-min Seikatsu*, **28**, 9-11 (2010).
- 12) National Consumer Affairs Center of Japan (NCAC), "Kurashi no Mamechishiki, 2011 edition," NCAC, Tokyo, 2010, p. 116.
- 13) Consumer Affairs Agency, Government of Japan: http://www.caa.go.jp/adjustments/pdf/110810_1.pdf, cited 19 April, 2012.
- 14) Office of Chemical Safety, Evaluation and Licensing Division, Pharmaceutical and Food Safety Bureau, Ministry of Health, Labour and Welfare: <http://www.mhlw.go.jp/stf/houdou/2r9852000001z31f.html>, cited 19 April, 2012.
- 15) Bureau of Citizens and Cultural Affairs, Tokyo Metropolitan Government: <http://www.metro.tokyo.jp/INET/CHOUSA/2010/10/60kap400.htm>, cited 19 April, 2012.
- 16) Isama K., Kawakami T., Nishimura T., *Yakugaku Zasshi*, **131**, 1135-1140 (2011).
- 17) Senga N., *Rep. Wakayama City Inst. Public Health*, **13**, 78-82 (2001, 2002).
- 18) Mitsuoka T., *Food Sanit. Res.*, **58**, 7-11 (2008).
- 19) Kawamura Y., *Food Sanit. Res.*, **58**, 13-17 (2008).
- 20) Toys "R" Us-Japan, Ltd.: <http://www2.toysrus.co.jp/truj/pdf/20080522.pdf>, cited 19 April, 2012.
- 21) MIKI SHOKO Co., Ltd., http://www.miki-house.co.jp/jp/news/new_080522.html, cited 19 April, 2012.
- 22) Isama K., Kawakami T., Tsuchiya T., Mitsuoka A., *J. Urban Living Health Assoc.*, **54**, 27-32 (2010).
- 23) Sakai S., Asari M., Sato N., Miyajima A., *J. Environ. Chem.*, **19**, 497-507 (2009).
- 24) Iizuka F., Hatano Y., Araki H., Shimada Y., Watanabe A., Ohisa K., Endo Y., Kuroki Y., Yoshioka T., *Jpn. J. Toxicol.*, **20**, 387-392 (2007).
- 25) Office of Chemical Safety, Evaluation and Licensing Division, Pharmaceutical and Food Safety Bureau, Ministry of Health, Labour and Welfare: <http://www.nihs.go.jp/mhlw/>

- chemical / katei / Pb / Pdhoukokusyohonbun.pdf), National Institute of Health Sciences Web, cited 19 April, 2012.
- 26) Centers for Disease Control and Prevention, U.S. Department of Health and Human Services. "Preventing Lead Poisoning in Young Children.": (<http://www.cdc.gov/nceh/lead/publications/PrevLeadPoisoning.pdf>), cited 19 April, 2012.
- 27) The U.S. Consumer Product Safety Commission. "Interim Enforcement Policy for Children's Metal Jewelry Containing Lead—2/3/2005.": (<http://www.cpsc.gov/BUSINFO/pbjewelgd.pdf>), cited 19 April, 2012.
- 28) The U.S. Consumer Product Safety Commission. "Standard operating procedure for determining lead (Pb) and its availability in children's metal jewelry—2/3/2005.": (<http://www.cpsc.gov/BUSINFO/pbjeweltest.pdf>), cited 19 April, 2012.
- 29) Isama K., Kawakami T., Tsuchiya T., Matsuoka A., *Yakugaku Zasshi*, **130**, 763–768 (2010).
- 30) The U.S. Consumer Product Safety Commission. "Section 101. Children's Products Containing Lead; Lead Paint Rule.": (<http://www.cpsc.gov/about/cpsia/sect101.html>), cited 19 April, 2012.

Genotoxicity of multi-walled carbon nanotubes in both *in vitro* and *in vivo* assay systems

Tatsuya Kato^{1,2}, Yukari Totsuka¹, Kousuke Ishino¹, Yoko Matsumoto^{1,3}, Yukie Tada⁴, Dai Nakae^{5,6}, Sumio Goto³, Shuichi Masuda², Sayaka Ogo⁷, Masanobu Kawanishi⁷, Takashi Yagi⁷, Tomonari Matsuda⁸, Masatoshi Watanabe⁹, & Keiji Wakabayashi²

¹Division of Cancer Development System, National Cancer Center Research Institute, Chuo-ku, Tokyo, Japan, ²Graduate School of Nutritional and Environmental Sciences, University of Shizuoka, Yada, Shizuoka, Japan, ³Laboratory of Environmental Risk Evaluation, School of Life and Environmental Science, Azabu University, Sagamihara, Kanagawa, Japan, ⁴Department of Environmental Health and Toxicology, Tokyo Metropolitan Institute of Public Health, Shinjuku-ku, Tokyo, Japan, ⁵Department of Pharmaceutical Sciences, Tokyo Metropolitan Institute of Public Health, Shinjuku-ku, Tokyo, Japan, ⁶Tokyo University of Agriculture, Setagaya-ku, Tokyo, Japan, ⁷Graduate School of Science, Osaka Prefecture University, Sakai, Osaka, Japan, ⁸Research Center for Environmental Quality Management, Kyoto University, Otsu, Shiga, Japan and ⁹Division of Materials Science and Engineering, Graduate School of Engineering, Yokohama National University, Hodogaya-ku, Yokohama, Japan

Abstract

The genotoxic effects of multi-walled carbon nanotubes (MWCNTs) were examined by using *in vitro* and *in vivo* assays. MWCNTs significantly induced micronuclei in A549 cells and enhanced the frequency of sister chromatid exchange (SCE) in CHO AA8 cells. When ICR mice were intratracheally instilled with a single dose (0.05 or 0.2 mg/animal) of MWCNTs, DNA damage of the lungs, analysed by comet assay, increased in a dose-dependent manner. Moreover, DNA oxidative damage, indicated by 8-oxo-7,8-dihydro-2'-deoxyguanosine and heptanone etheno-deoxyribonucleosides, occurred in the lungs of MWCNT-exposed mice. The *gpt* mutation frequencies significantly increased in the lungs of MWCNT-treated *gpt* delta transgenic mice. Transversions were predominant, and G:C to C:G was clearly increased by MWCNTs. Moreover, many regions immunohistochemically stained for inducible NO synthase and nitrotyrosine were observed in the lungs of MWCNT-exposed mice. Overall, MWCNTs were shown to be genotoxic both in *in vitro* and *in vivo* tests; the mechanisms probably involve oxidative stress and inflammatory responses.

Keywords: micronuclei, sister chromatid exchange, DNA damage, *gpt* mutation, oxidative stress

Introduction

Multi-walled carbon nanotubes (MWCNTs) are among the most extensively researched and developed nanomaterials, finding use in electrochemical devices and for many biomedical applications. Accordingly, the market for MWCNTs

is predicted to grow on a global scale and would be released into the human environment and subsequent inhalation would occur, especially in workplaces. Since MWCNTs are not only nanosized particles, but also rod-shaped fibres with a superbly high aspect ratio, their carcinogenic potential have attracted attention over the years. In fact, mesothelioma could be induced by a single intraperitoneal administration of MWCNTs in both cancer susceptible *p53*^{+/-} mice and F344 rats (Takagi et al. 2008; Sakamoto et al. 2009). Although intraperitoneal application is not relevant to human exposure, the findings point to possible major hazard.

Due to high cost and the need for special equipment for inhalation studies to create mock conditions for the situation of human exposure, only a few reports on MWCNT inhalation are available so far (Porter et al. 2010; Morimoto et al. 2011). On the other hand, intratracheal instillation is less expensive and more easily performed, and there have been several reports of MWCNT exposure by this route using rats (Takaya et al. 2010; Reddy et al. 2012; Morimoto et al. 2011). MWCNTs induced strong inflammatory reactions, including formation of granulomas and fibrosis in the lungs. Translocation into lung-associated lymph nodes was also observed in mice and rats with both inhalation and intratracheal exposure (Porter et al. 2010, 2002; Ellinger-Ziegelbauer & Pauluhn 2009; Pauluhn 2010a). In addition to MWCNT-induced pulmonary toxicity, genotoxicity, such as micronucleus induction, chromosome aberration and DNA damage, using *in vitro* and *in vivo* assay systems have been reported and are a little controversial (Wirnitzer et al. 2009; Asakura et al. 2010; Ghosh et al. 2011; Patlolla et al. 2010a,b,c; Migliore et al. 2010). For example, Wirnitzer et al. reported

that MWCNTs demonstrated neither cytotoxic, clastogenic activities against mammalian cells nor bacteriotoxic, mutagenic activities for bacterial strains. However, most reports revealed that MWCNTs, indeed, are genotoxic and clastogenic for cultured mammalian cells, plants and mice. Among these, chromosomal damage by carbon nanotubes (both single-wall and multi-wall) has been well documented (Asakura *et al.* 2010; Muller *et al.* 2008; Sargent *et al.* 2009, 2011 unpublished data). However, *in vivo* genotoxicity including mutagenicity of MWCNTs has not been fully elucidated yet.

The present study, therefore, aimed to examine the genotoxicity/clastogenicity of this nanomaterial, MWCNTs, in both *in vitro* micronucleus and sister chromatid exchange (SCE) tests. Genotoxic effects were also examined by *in vivo* comet assay, DNA adduct formation and mutation assay using wild type and transgenic mice. In the present study, MWCNTs were, thereby, demonstrated to be genotoxic both in *in vitro* and *in vivo* tests, and possible mechanisms were also suggested. Finally, health concerns raised by the use of MWCNTs are also discussed.

Materials and methods

Materials

High-purity MWCNTs (MITSUI MWCNT-7, identical to those used in the Fischer 344 rats study of Sakamoto *et al.* 2009) were provided by Mitsui & Co., Ltd. (Ibaraki, Japan). MWCNTs were suspended in saline containing 0.05% Tween 80 (Nacalai Tesque, Kyoto, Japan) and sonicated well on ice. Width distribution of MWCNTs used in the present study indicated a Gaussian distribution with a peak at 90 nm, and more than 80% of particles belonged in a range of 70–110 nm. The length of MWCNTs distributed with a peak at 2 μm , and more than 70% of particles belonged in a range of 1–4 μm (Sakamoto *et al.* 2009). Detailed information, such as elemental contents of MWCNTs, can be found in a previous report (Sakamoto *et al.* 2009).

Standards of DNA adducts and their stable isotopes

8-Oxo-7,8-dihydro-2'-deoxyguanosine (8-oxodG) was purchased from Sigma-Aldrich Japan (Tokyo, Japan). [$^{15}\text{N}_5$]-8-oxodG was supplied by Dr Shibutani at SUNY Stony Brook, NY, USA. 4-Oxo-2(*E*)-nonenal-derived DNA adducts, heptanone etheno-2'-deoxycytidine (HedC), heptanone etheno-2'-deoxyguanosine (HedG) and heptanone etheno-2'-deoxyadenosine (HedA) were synthesised according to previously published methods (Rindgen *et al.* 1999, 2000; Pollack *et al.* 2003).

Micronucleus test

A micronucleus test using human lung carcinoma A549 cells (RIKEN Cell Bank, Wako, Japan) was performed, as described previously (Totsuka *et al.* 2009). Briefly, A549 cells were seeded in plastic cell culture dishes ($\phi 60$ mm) 1 day before treatment. Particles were suspended in physiological saline containing 0.05% (v/v) Tween-80 with sonication (for 5–10 min at room temperature). One volume of the suspension was mixed with nine volumes of the

culture medium with serum (altogether 3.3 mL/dish), and then cells were treated at indicated concentrations for 6 h. After treatment, cells were further cultured for 42 h. Then, cells were trypsinized and counted and centrifuged. Cells were resuspended in 0.075 M KCl, and incubated for 5 min. Cells were then fixed four times in methanol:glacial acetic acid (3:1) and washed with methanol containing 1% acetic acid. Finally, cells were resuspended in methanol containing 1% acetic acid. The cell solution was dropped onto slides and the nucleus was stained by mounting with 40 $\mu\text{g}/\text{mL}$ acridine orange (Nacalai Tesque) solution and immediately observed by fluorescence microscopy using blue excitation. The number of cells with micronuclei was recorded based on observation of 1000 interphase cells.

SCE test

Chinese hamster ovary (CHO) AA8 cells were cultured in RPMI 1640 (Sigma-Aldrich, Japan) supplemented with 10% foetal bovine serum (JRH Biosciences, Lenexa, KS) in a 5% CO_2 atmosphere at 37°C. The cells were treated with MWCNTs for 1 h and cultured in medium containing 10% serum and 10 $\mu\text{g}/\text{mL}$ 5-bromodeoxyuridine (Sigma-Aldrich, Japan) for 26 h. Colcemid (Nacalai Tesque) was added for the last 2 h at a final concentration of 60 ng/mL. Cells were trypsinized and centrifuged, resuspended in 0.075 M KCl, and incubated for 30 min. The cells were fixed four times in methanol:glacial acetic acid (3:1). The cell solution was dropped onto slides in a Metaphase Spreader HANABI (AD Science Technology, Funabashi, Japan). The slides were soaked in 50 $\mu\text{g}/\text{mL}$ Hoechst #33258 (Sigma-Aldrich, St. Louis, MO, USA). The slides were covered with 0.01 M sodium phosphate buffer (pH 7.6) and cover glasses and irradiated with black light at 365 nm for 3 h. Subsequently, slides were stained with 6% Giemsa (Merck KGaA, Darmstadt, Germany) in 0.06 M sodium phosphate buffer (pH 6.4) for 15 min. SCE was scored under a microscope. The experiments were repeated until acquiring at least 50 cells that were suitable for scoring SCEs in each dose.

Animals

Male ICR mice (6 weeks old) and guanine phosphoribosyltransferase (*gpt*) delta mice (9 weeks old) were purchased from Japan SLC (Shizuoka, Japan). The *gpt* delta mice carry ~80 copies of *lambda* EG10 DNA on each chromosome 17 on a C57BL/6J background (Nohmi & Masumura 2005). The animals were provided with food (CE-2 pellet diet; CLEA Japan, Inc., Tokyo, Japan) and tap water *ad libitum* and maintained under controlled conditions: a 12 h light/dark cycle, 22 \pm 2°C room temperature and 55 \pm 10% relative humidity. After quarantine for 1 week, the experiments were conducted according to the "Guidelines for Animal Experiments in the National Cancer Center" of the Committee for Ethics of Animal Experimentation of the National Cancer Center.

In vivo comet assay

Each group of five male ICR mice was intratracheally instilled with nanoparticles using a polyethylene tube under anaesthesia with 4% halothane (Takeda Chemical,

Table I. Sister chromatid exchange (SCE) in CHO AA8 cells following a 1 h treatment with MWCNTs.

Treatment [$\mu\text{g}/\text{mL}$]	SCEs/cell*
0 [†]	3.87 \pm 1.82
0.1	6.65 \pm 1.30 [‡]
1.0	11.3 \pm 2.58 [‡]
2.0	10.1 \pm 1.52 [‡]

*Mean \pm SD of at least 50 cells; [†]Solvent control (treatment with 0.05% (v/v) Tween 80); [‡] $p < 0.01$ (versus solvent control) by Student's *t*-test.

Osaka, Japan). Single doses of 0.05 or 0.2 mg/animal were employed. The control mice ($n = 5$) were instilled intratracheally with 0.1 mL of the solvent alone. The mice were sacrificed 3 h after particle administration; the lungs were removed and then used immediately for comet analysis. The alkaline comet assay was performed according to previously described procedures (Totsuka et al. 2009). Fifty cells were examined per mouse. The tail moment of DNA was automatically measured using a Comet Analyzer from Youworks Co. (Ibaraki, Japan). The distance between the centre of nucleus and centre of tail was defined as tail distance, and the fluorescence intensity of damaged area was divided by that of the whole area of cell to achieve the damage ratio. The tail moment was calculated by multiplication of tail distance and damage ratio. Furthermore, percentage of DNA in the tail, another index of DNA damage, was also calculated.

DNA adduct analysis

For DNA adduct analyses, each group of five male ICR mice was intratracheally instilled with MWCNTs at a single dose of 0.2 mg/animal, and sacrificed 3, 24, 72 or 168 h after nanoparticle administration. Control samples were obtained from the lungs of mice given vehicle. Mouse lung DNA was extracted and purified using a Genra[®] Puregene[™] tissue kit (QIAGEN, Valencia, CA, USA). The protocol was performed according to the manufacturer's instructions except that desferroxamine (final concentration: 0.1 mM) was added to all solutions to avoid the formation of oxidative adducts during the purification step.

DNA samples in 40 μg aliquots were digested into their constituent 2'-deoxyribonucleoside-3'-monophosphate units by the addition of 15 μL of 17 mM citrate plus 8 mM CaCl_2 buffer that contained micrococcal nuclease (22.5 U) and spleen phosphodiesterase (0.075 U) plus internal standards. The solutions were mixed and incubated for 3 h at 37°C, then alkaline phosphatase (1 U), 10 μL of 0.5 M Tris-HCl (pH 8.5), 5 μL of 20 mM ZnSO_4 and 67 μL of distilled water were added and the reactions were incubated for a further 3 h at 37°C. The digested sample was extracted twice with methanol. The methanol fractions were evaporated to dryness, resuspended in 50 μL of distilled water and subjected to liquid chromatography tandem mass spectrometry (LC/MS/MS). LC/MS/MS analyses were performed using a Waters 2795 LC system (Waters, Manchester, UK) interfaced with a Quattro Ultima triple stage quadrupole MS (Waters). The LC column was eluted over a gradient that began at a ratio of 5% methanol to 95% water, changed to 30% methanol over a period of 30 min, changed to 85% methanol from 30 to 45 min, and was then maintained at 85% methanol from 45 to 55 min. Sample

injection volumes of 20 μL each were separated on a Shim-pack FC-ODS column (150 \times 4.6 mm, 3 μm , Shimadzu, Kyoto, Japan) and eluted at a flow rate of 0.4 mL/min. Mass spectral analyses were carried out in positive ion mode with nitrogen as the nebulising gas. The ion source temperature was 130°C; the desolvation gas temperature was 380°C. Nitrogen gas was also used as the desolvation gas (700 L/h) and cone gas (35 L/h) and argon was used to provide a collision cell pressure of 1.5×10^{-3} mbar. Positive ions were acquired in multiple reaction monitoring mode. The multiple reaction monitoring transitions were monitored; each cone voltage and collision energy used was as follows: 8-oxodG [284->168, 35 V, 14 eV], HedG [404->288, 35 V, 10 eV], HedA [388->272, 35 V, 10 eV], HedC [364->248, 35 V, 10 eV].

gpt and *Spi*⁻ mutation assays

For mutation analysis, each group of six to seven male *gpt* delta mice was intratracheally instilled with particles at a single dose or multiple doses of 0.2 mg/animal as follows. Group 1 served as the vehicle control (0.1 mL of saline containing 0.05% Tween 80), Groups 2–4 were the study groups and received single or multiple doses of MWCNTs (Group 2: single dose of 0.2 mg/animal; Group 3: 0.2 mg/animal for each of two instillations 2 weeks apart; Group 4: 0.2 mg/animal, once a week for 4 weeks). The mice were sacrificed at 22 weeks of age; this was 8–12 weeks after particle administration. Lungs were removed, and stored at -80°C until high-molecular-weight genomic DNA was extracted using a RecoverEase DNA Isolation Kit (Stratagene, La Jolla, CA, USA), according to the manufacturer's instructions. *Lambda* EG10 phages were rescued using Transpack Packaging Extract (Stratagene). The *gpt* and *Spi*⁻ mutagenesis assay was performed, according to previously described methods (Nohmi et al. 2000).

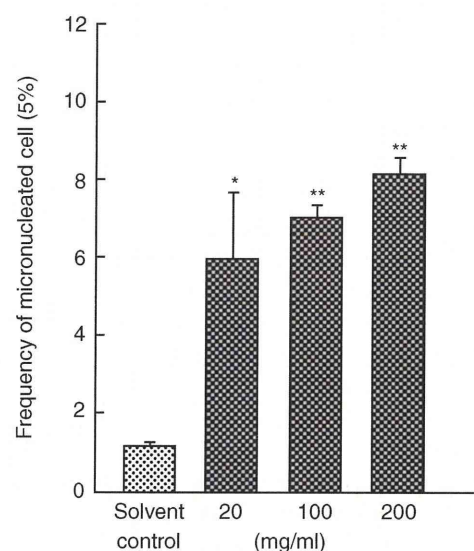


Figure 1. Frequency of micronucleated A549 cells. The frequency was calculated after counting the number of cells with micronuclei based on observation of 1000 interphase cells. Mean values \pm SD of three independent experiments are shown. Solvent control represents treatment with 0.05% (v/v) Tween 80; * $p < 0.05$ and ** $p < 0.01$, by Student's *t*-test.

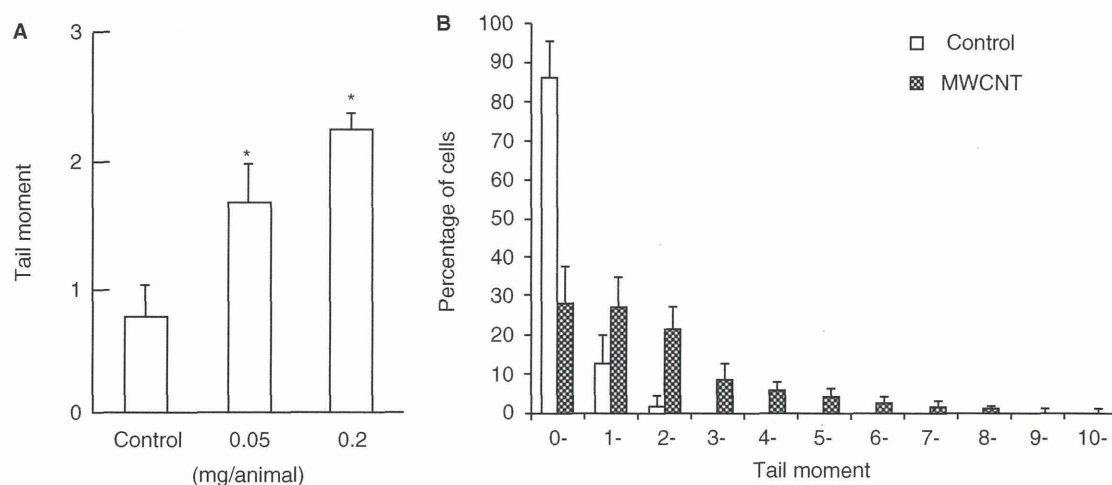


Figure 2. DNA damage in the lungs of ICR mice intratracheally instilled with MWCNTs. DNA damage was measured by comet assay. (A) The mean values of DNA tail moment in the lungs with or without a 3 h MWCNT treatment at 0.05 or 0.2 mg/animal. The values represent the mean of five animals \pm SD; * $p < 0.01$, by Dunnett's test after one-way analysis of variance versus the corresponding vehicle control mice. (B) The percentages of cells containing a given comet tail moment at a dose of 0.2 mg/animal.

Histopathological evaluation

For histopathological evaluation, lungs obtained from *gpt* delta mice with or without nanoparticle instillation ($n = 2$ or 3) were fixed in 10% neutral buffered formalin, embedded in paraffin blocks, and routinely processed to haematoxylin and eosin-stained sections.

Immunohistochemical analysis of inflammation factors

To investigate nitric oxide production after nanoparticle exposure, immunohistochemical staining of inflammation factors, such as inducible NO synthase (iNOS) and nitrotyrosine (NT), in the lungs of *gpt* delta mice treated with MWCNTs were examined, using a procedures reported previously (Totsuka et al. 2010; Porter et al. 2002).

Statistical analysis

The data obtained from the comet assay were expressed as the mean \pm standard deviation (SD). Dunnett's test after one-way analysis of variance was used to test for significant differences in tail moment and percentage of DNA in tail. The data from the micronucleus test were expressed as the mean \pm SD of three independent experiments. The data from the SCE test were expressed as the mean \pm SD of at least 50 cells. The data from the *gpt* and *Spi*⁻ mutation assays were expressed as the mean \pm SD. The data were statistically compared with the corresponding solvent control using the F test before application of the Student's *t*-test. Mutational spectra were compared using Fisher's exact test (Carr & Gorelick 1996). *P* values < 0.05 were considered to indicate statistical significance.

Results

Micronucleus test

To investigate the genotoxicity/clastogenicity of MWCNTs, micronucleus-inducing activity was analysed using a human lung cancer cell line, A549. A 6 h treatment with MWCNTs, at a concentration of 20 μ g/mL or higher, inhibited A549 cell growth to around 70% of control levels. As shown in Figure 1,

MWCNTs increased the number of micronucleated cells in a dose-dependent manner. The frequency of micronucleated cells in the solvent control was 1.12% and the frequency rose to 8.6% in the 200 μ g/mL MWCNT group. Even treatment of 20 μ g/mL MWCNT induced micronuclei exceedingly, and these increases were statistically significant ($p < 0.05$).

SCE test

Table I shows the SCE frequency in CHO cells following a 1 h treatment with MWCNTs. An SCE frequency approximately three times the control level was observed in cultures treated with 1.0 μ g/mL MWCNTs. This increase was statistically significant ($p < 0.01$) at 0.1 μ g/mL or higher concentrations.

In vivo genotoxicity analysed by alkaline comet assay

DNA damage induced by MWCNTs in the lungs was evaluated using a comet assay under alkaline conditions. Figure 2A shows the mean values of DNA tail moment in the lungs with or without a 3 h MWCNT treatment at 0.05 or 0.2 mg/animal. DNA damage observed in the MWCNT-treated group was dose-dependent, and the values of DNA tail moment were significantly increased compared with those of the vehicle control. Also, similar dose-dependent manner was observed in the values of percentage of DNA in the tail (Supplementary Figure 1). Figure 2B shows the percentages of cells containing a given comet tail moment at a dose of 0.2 mg/animal. The numbers of damaged cells were increased by treatment with nanoparticles and damaged cells with high DNA tail moment being extremely rare in the vehicle group.

Quantification of oxidative and lipid peroxide-related DNA adducts

Levels of the DNA adduct analysed in lung DNA extracted from MWCNT-treated mice at 3, 24, 72 and 168 h after exposure are shown in Figure 3. DNA adducts related to oxidative stress and lipid peroxidation (8-oxodG, H ϵ dA, H ϵ dC, H ϵ dG) were all, except H ϵ dG, increased up to 72 h and then slightly less so at 168 h. 8-OxodG was more

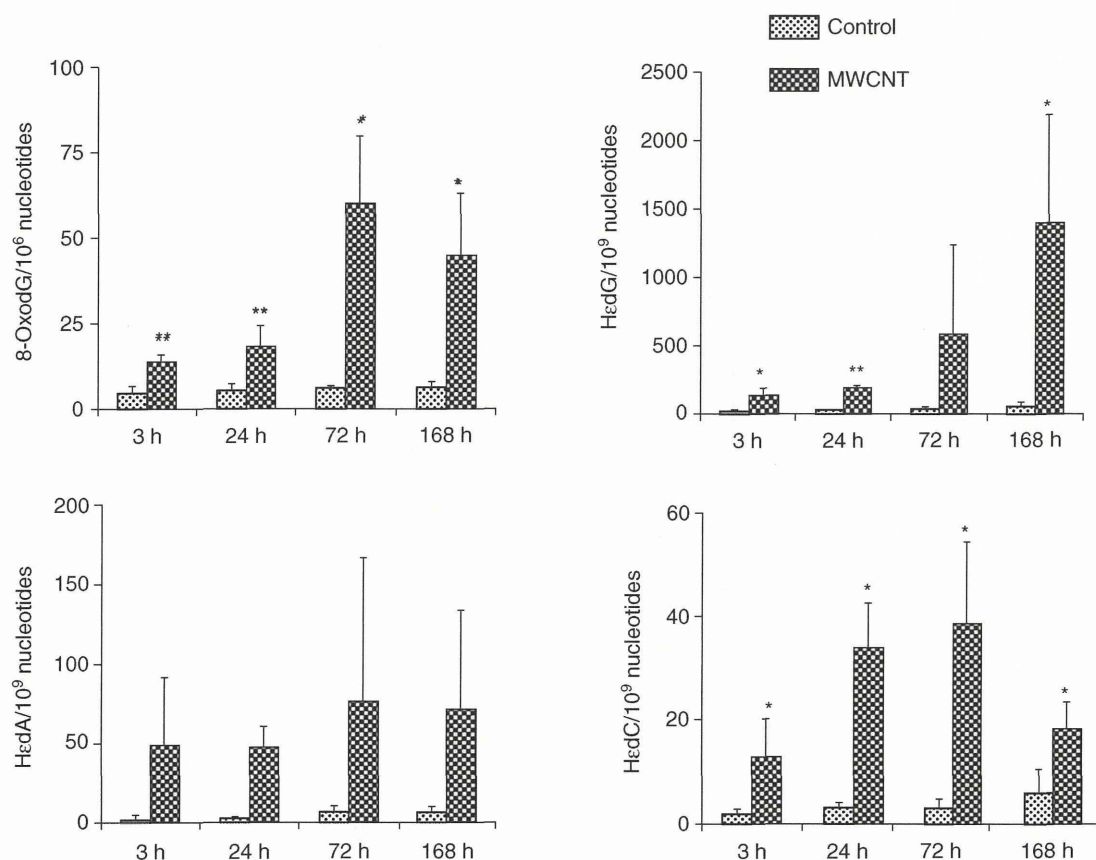


Figure 3. Oxidative and lipid peroxide-related DNA adduct formation induced by MWCNT exposure in the lungs of ICR mice. DNA was extracted from the lungs 3, 24, 72 and 168 h after intratracheal instillation of 0.2 mg of MWCNTs, and was enzymatically digested. Control samples were obtained from the lungs of mice given vehicle for the same durations of MWCNT exposure. 8-OxodG and three types of Hε-adduct were quantified by stable isotope dilution LC-MS/MS. Asterisks (*, **) indicate a significant difference ($p < 0.05$, < 0.01) from vehicle control (treatment with 0.05% (v/v) Tween-80) at same point in the Student's *t*-test.

abundantly found than the Hε-adduct derived from lipid peroxidation.

General observations and histopathological evaluation of *gpt* delta transgenic mice administered with MWCNTs

The body weights of *gpt* delta mice in the vehicle control group were 34.9 ± 1.9 g at the end of the experiment. The body weights of the *gpt* delta mice that received single or multiple doses of 0.2 mg MWCNTs were 75–80% of those in the vehicle control group during or just after the instillations, then gradually returned to normal by the end of the experiment.

There were no obvious histopathological changes in the lungs of Group 1 control mice (Figure 4A). In mice given a single MWCNT administration (0.2 mg/animal; Group 2), infiltration of macrophages phagocytosing tubes in the alveolar lumina and walls, and granulation with fibrosis were observed, in association with inflammatory lymphocyte infiltration in macrophage-clustered lesions and around the vessels and bronchi (Figure 4B). Degeneration, enhanced secretion and hyperplasia were found in the bronchial epithelia, and type II alveolar epithelial cells appeared hyperplastic (Figure 4B). The thickening lesions were also seen in the visceral pleurae, which were due to sub-pleural fibrosis with the occasional detection of MWCNTs (Figure 4D and 4E). When MWCNTs were multiply administered (0.2 mg

weekly for 4 weeks; Group 4), generally similar findings were observed but with a much higher severity (Figure 4C). Moreover, MWCNTs were deposited in the paratracheal lymph nodes (Figure 4F). Similar findings, but with a slighter degree of particle accumulation and granuloma formation, were observed in the lungs of mice that received two consecutive MWCNT instillations (Group 3; data not shown).

gpt and *Spi*⁻ mutations in the lungs of *gpt* transgenic mice treated with MWCNTs

The *gpt* delta transgenic mice were exposed to single or multiple intratracheal instillations of 0.2 mg MWCNTs and the mutations in the lungs were analysed. Data are summarised in Supplementary Table I, and Figure 5 shows the *gpt* mutant frequencies (MFs) in the lungs. The background MF of the lungs was $7.53 \pm 0.91 \times 10^{-6}$. There was no increase in the MF in lungs exposed to single or double doses of MWCNTs. However, four instillations of MWCNTs resulted in a significant increase in the MF, of approximately two-fold compared with that in controls (Figure 5). The *Spi*⁻ MFs were measured in the lungs of *gpt* delta mice instilled with MWCNTs, but no increases were observed (data not shown).

To analyse the characteristics of the mutations induced by MWCNTs, the authors tested for 6-thioguanine (6-TG)-resistant mutants using PCR and DNA sequencing analysis. A total of 42 independent 6-TG-resistant mutants derived

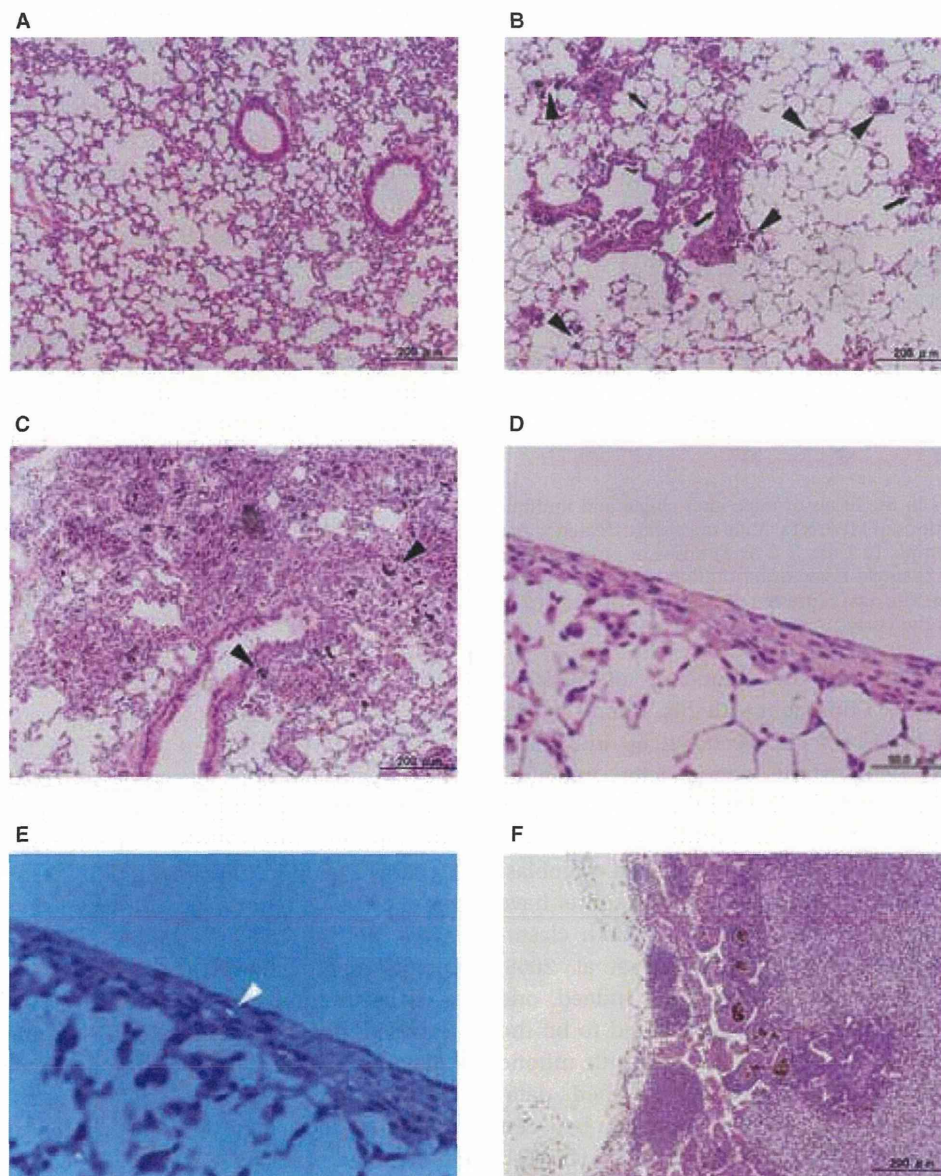


Figure 4. Representative histopathology of the lungs of (A) a control mouse given vehicle (once a week for 4 weeks; killed at the end of month 3); (B) a mouse given a single dose of 0.2 mg MWCNTs (killed at the end of month 3); (C) a mouse given multiple doses of 0.2 mg MWCNTs (once a week for 4 weeks; killed at the end of month 3); (D) a mouse given MWCNT (0.2 mg/head, singly, killed at the end of month 3); (E), a polarisation photomicrograph serial to (D); and (F) a representative paratracheal lymph node of a mouse given multiple doses of 0.2 mg MWCNTs (once a week for 4 weeks; killed at the end of month 3). MWCNT-phagocytised macrophages (black arrowheads) can be observed, and granulation with fibrosis (black arrows) is also found in lungs of MWCNT-instilled mice. In polarisation photomicrograph, MWCNTs is indicated by white arrowhead.

from MWCNT instillations were identified and 24 mutants were identified from vehicle controls. The classes of mutation found in the *gpt* gene are summarised in Table II. Base substitutions predominated in nanoparticle-induced and spontaneous cases. No G:C to C:G transversions were detected in the vehicle control group; however, this type of mutation could be detected in several MWCNT-instilled animals, and p value can be considered significant ($p < 0.05$). The numbers of A:T to T:A transversions and deletions were also slightly increased by MWCNT treatment, though p values were not significant.

Immunohistochemical analysis of inflammation factors

As shown in Figure 6, the pattern of iNOS and NT staining corresponded to the areas of inflammation within the lung

parenchyma. In the case of MWCNT exposure, many regions of the lungs stained positively, and intense iNOS and NT staining was mainly localised in test substance-phagocytised macrophages and granulomas (indicated by green arrows). Some alveolar epithelial cells located near granulomas were also stained positive for the iNOS and NT antibodies (indicated by arrowheads). In contrast, no regions stained positively for iNOS were observed in the lungs of vehicle control mice (Figure 6D). Similar results were obtained for vehicle control mice immunoreaction with NT (data not shown).

Discussion

The present study showed MWCNTs to clearly exert genotoxicity in *in vitro* assay systems, significantly inducing

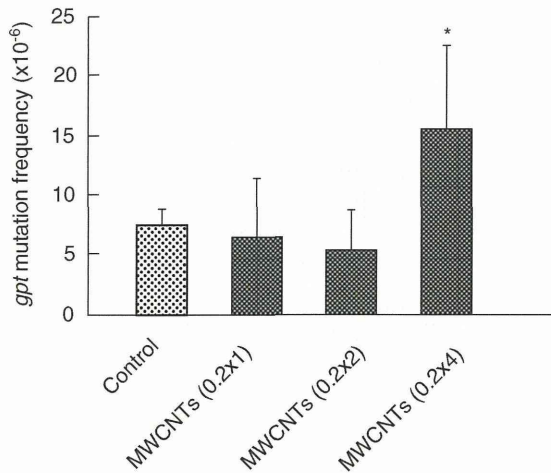


Figure 5. The *gpt* MFs in the lungs of mice after single and multiple intratracheally instillations of MWCNTs. Male mice were treated with a single (0.2 mg) or multiple (0.2 mg × 2 or 4) doses of particles, and mice were sacrificed 12 (single-dose) or 8 (multiple-dose) weeks after particle administration. The data represent the mean ± SD; **p* < 0.05 by Student's *t*-test versus the corresponding vehicle control mice.

micronuclei and enhancing the frequency of SCEs in A549 and CHO AA8 cells. Consistent with this, several studies have reported that MWCNTs can be taken up into many types of cells and demonstrate genotoxicity, including human epithelial lung cells (Wörle-Knirsch et al. 2006), mesothelioma cells (Wick et al. 2007), keratinocytes (Monteiro-Riviere et al. 2005), and normal dermal fibroblast cells (Patlolla et al. 2010b). Recently, several reports have demonstrated that carbon nanotubes induce both clastogenic events and aneugenic events (Muller et al. 2008; Sargent et al. 2009, 2011 unpublished data). Indeed, one of the mechanisms of genotoxicity is considered to be the disruption of mitotic spindles by association with mitotic tubules (Sargent et al. 2009, 2011 unpublished data; Asakura et al. 2010). Moreover, a direct interaction between carbon nanotubes and DNA has also been reported (Li et al. 2005). Other than that, it has been reported that modified gold nanoparticles induce the unfolding of fibrinogen *via* binding and then promote interaction with the integrin

receptor Mac1 and induce the release of inflammatory cytokines (Deng et al. 2011). In the present study, no data are available to explain the exact mechanisms of *in vitro* genotoxicity by MWCNTs; however, direct interaction between biomolecules, such as protein and DNA, and MWCNTs might be partly involved for induction of the *in vitro* genotoxicity.

In addition to the *in vitro* genotoxicity, MWCNTs were showed to be genotoxic in the lungs of mice using a comet assay. Under similar conditions, levels of 8-oxodG were significantly increased in MWCNT-treated mice, and the level was maintained for 1 week. The levels of H_{ed}A, H_{ed}C and H_{ed}G also tended to increase. These DNA adducts are derived from lipid peroxidation, suggesting that MWCNTs may induce oxygenation of lipids in tissues caused by generation of reactive oxygen species (ROS). Consistently, it has been reported that the levels of lipid hydroperoxides, which are prominent non-radical intermediates of lipid peroxidation products, were increased in the liver of Swiss-Webster mice intraperitoneally administered with MWCNTs (Patlolla et al. 2010c). Moreover, in the present study, MWCNTs showed mutagenicity in the lungs of *gpt* delta transgenic mice. However, a dose-dependent MF increase was not observed in the lungs of MWCNT-treated groups. The reason is still unclear, but weak responses observed in single or double doses suggested that the degree of DNA damage seems insufficient to fix as mutations, therefore it could not raise MFs more than basal levels under these conditions. Supporting this hypothesis, previous reports have revealed that obvious responses were not observed in either cellular inflammatory end points in bronchoalveolar lavage or pathological changes, such as immune response and fibrosis, in the lungs of animals exposed to low doses of MWCNTs (Ryman-Rasmussen et al. 2009; Pauluhn 2010a). On the other hand, it has also been reported that MWCNTs are difficult to eliminate; it remain in the lungs for a long time and trigger sustained pulmonary inflammation (Ellinger-Ziegelbauer & Pauluhn 2009; Pauluhn 2010a,b). Therefore, to evaluate the effects of MWCNTs with low exposure, it would be preferable to use long-term mutation assay systems. In general, 8-oxodG causes transversion

Table II. Classification of *gpt* mutations isolated from the lungs of control and MWCNT-treated mice.

Type of mutation	Control		MWCNTs		<i>p</i> value*
	No. of mutants (%)	Specific MF [†] (× 10 ⁻⁶)	No. of mutants (%)	Specific MF [†] (× 10 ⁻⁶)	
Base substitution					
Transition					
G:C to A:T	7 (29.2)	2.20	11 (26.2)	4.03	0.238
A:T to G:C	2 (8.3)	0.62	2 (4.8)	0.74	1.000
Transversion					
G:C to T:A	8 (33.3)	2.51	10 (23.8)	3.66	0.481
G:C to C:G	0 (0)	0.00	5 (11.9)	1.83	0.02
A:T to T:A	0 (0)	0.00	1 (2.4)	0.37	0.458
A:T to C:G	2 (8.3)	0.62	2 (4.8)	0.74	1.000
Insertion	1 (4.2)	0.32	2 (4.8)	0.74	0.596
Deletion	4 (16.7)	1.26	9 (21.4)	3.29	0.101
Others	0 (0)	0.00	0 (0)	0.00	-
Total	24 (100)	7.53	42 (100)	15.40	0.004

**p* values were determined using Fisher's exact test according to Carr and Gorelick; [†]Specific MF was calculated by multiplying the total mutation frequency by the ratio of each type of mutation to the total mutation.